Bioorganic Chemistry 40 (2012) 114–124

Contents lists available at SciVerse ScienceDirect

Bioorganic Chemistry

journal homepage: www.elsevier.com/locate/bioorg

Monoamine oxidase inhibition by C4-substituted phthalonitriles

Clarina I. Manley-King, Jacobus J. Bergh, Jacobus P. Petzer *

Pharmaceutical Chemistry, School of Pharmacy, North-West University, Private Bag X6001, Potchefstroom 2520, South Africa

ARTICLE INFO

Article history:
Received 13 September 2011
Available online 29 October 2011

Keywords:
Monoamine oxidase
Reversible inhibition
Phthalonitrile
Phthalimide
Benzonitrile
Molecular docking

ABSTRACT

It was recently reported that a series of C5-substituted phthalimides are remarkably potent reversible inhibitors of recombinant human monoamine oxidase (MAO) B. Modeling studies suggested that the phthalimide ring forms numerous polar interactions with the polar region of the MAO-B substrate cavity while the C5 side chain extends to, and interacts via Van der Waals interactions with the hydrophobic regions of the enzyme entrance cavity. Interactions with both cavities appear to be requirements for high affinity binding. In the present study we have examined an analogs series of C4-substituted phthalonitriles as potential human MAO inhibitors. The phthalonitriles were found to be highly potent reversible MAO-B inhibitors with most analogs exhibiting IC_{50} values in the low nM range. The phthalonitriles also interacted with human MAO-A, although with lower binding affinities compared to MAO-B. Modeling studies suggest that the high binding affinities of the phthalonitriles to MAO-B may depend, at least in part, on the formation of polar interactions between the nitrile functional groups and the enzyme substrate cavity. Examination of a homologs series of benzonitriles established that the phthalonitrile moiety is more optimal for MAO-B inhibition than the corresponding benzonitrile moiety, and that C3-substituted benzonitriles are better MAO-B inhibitors than C4-substituted benzonitriles. Since elimination of the nitrile functional group yielded compounds with only moderate MAO-B inhibition potencies, it may be concluded that this functional group is privileged for MAO-B inhibition.

1. Introduction

Monoamine oxidase A and B (MAO-A and -B) play essential roles in the oxidation of neurotransmitter amines in the brain and peripheral tissues [1]. MAO-A selectively catalyzes the oxidation of serotonin while dopamine, epinephrine and norepinephrine are substrates for both MAO isoforms [2]. The false neurotransmitters, benzylamine and β-phenylethylamine, are metabolized by MAO-B [2,3].

Based on their roles in the catabolism of monoamine neurotransmitters, the MAO enzymes are considered to be useful drug targets [2,4,5]. Since both MAO isoforms are found in the human brain, inhibitors of these enzymes are employed in neuropsychiatric and neurodegenerative diseases [6,7]. MAO-A inhibitors are used in the treatment of anxiety disorder and depressive illness [2,8]. MAO-B inhibitors, in turn, reduce the catabolism of dopamine in the basal ganglia and are employed in the treatment of Parkinson's disease [9,10]. MAO-B inhibitors not only prolong the action of dopamine in the brain, but also enhance dopamine levels after treatment with levodopa, the metabolic precursor of dopamine [11,12]. For these reasons, MAO-B inhibitors are frequently combined with levodopa in Parkinson's disease therapy [5,10]. Interestingly, MAO-B inhibitors are also thought to protect against the neurodegenerative processes associated with Parkinson's disease [13]. This effect may, in part, be attributed to the reduction of harmful metabolic by-products such as dopanal and H_2O_2 that arise from the MAO-B catalyzed oxidation of dopamine [14–18]. Of significance is the observation that MAO-A activity remains constant with age while MAO-B levels and activity increase up to 4–5 fold in most brain regions, including the basal ganglia [19–21]. In the aged parkinsonian brain, the inhibition of MAO-B catalyzed dopamine turnover may therefore be particularly relevant since it would lead to a reduction of harmful dopamine-derived oxidation products and possibly protection against further neuronal damage.

The availability of the three-dimensional structures of both MAO-A and -B greatly assists in the design of new inhibitors of these enzymes [22,23]. The active site of MAO-A consists of a single cavity while the active site of MAO-B is comprised of two separate spaces, an entrance cavity and substrate cavity [22]. The MAO-B active site cavities are normally separated by the side chain of Ile-199, but upon binding of larger cavity-filling ligands, the

Abbreviations: CCDC, Cambridge crystallographic data centre; DMSO, dimethyl sulfoxide; FAD, flavin adenine dinucleotide; MAO, monoamine oxidase; PDB, protein data bank; RMSD, root mean square deviation.

* Corresponding author. Fax: +27 18 2994243.
E-mail address: jacques.petzer@nwu.ac.za (J.P. Petzer).

0045-2068/$ - see front matter © 2011 Elsevier Inc. All rights reserved.
doi:10.1016/j.bioorg.2011.10.003

Ile-199 may adopt an alternate conformation which allows for the fusion of the two cavities [24]. X-ray crystallography has shown that relatively large MAO-B inhibitors, such as safinamide (**1**) (Fig. 1), adopt an orientation in the active site that places the polar end of the molecule, the propanamidyl moiety, in the polar region of the substrate cavity, near the FAD, while the apolar fluorobenzyloxy side chain extends into the hydrophobic entrance cavity [25]. This dual interaction mode may, to a large degree, explain the high binding affinity of safinamide for the MAO-B active site. Several other examples exist of relatively large cavity-filling MAO-B inhibitors which undergo polar and apolar interactions with the substrate and entrance cavities, respectively. For example, the chlorobenzyloxy side chain of 7-(3-chlorobenzyloxy)-4-formylcoumarin (**2**) binds in the entrance cavity of the enzyme with the polar coumarin ring interacting with the polar region of the substrate cavity [25]. A recent report documents that a series of C5-substituted phthalimides (**3**) are exceptionally potent reversible inhibitors of recombinant human MAO-B [26]. Modeling studies suggested that the polar functional groups of the phthalimide ring forms numerous interactions with the polar region of the MAO-B substrate cavity while the apolar C5 side chain extends to, and interacts via Van der Waals interactions with the hydrophobic entrance cavity of the enzyme. Similar to safinamide, interactions with both the substrate and entrance cavities may explain the high binding affinities of the C5-substituted phthalimides to MAO-B. Based on the MAO inhibition properties of the phthalimides, in the present study a homologs series of C4-substituted phthalonitriles (**4**) were synthesized and examined as potential human MAO-A and -B inhibitors (Fig. 2). With the selection of C4 side chains of relatively low polarity suited for binding within the entrance cavity, the C4-substituted phthalonitriles may exhibit high binding affinities to MAO-B since the nitrile functional group is highly polar and may interact with the polar regions in the substrate cavity. These compounds may therefore also exhibit a dual mode of binding to the MAO-B active site, a property which is thought to be favorable for high affinity binding. The notion that nitriles may undergo polar interactions with the active site of MAO-B is supported by the observation that the nitrile functional group is considered to be a bioisostere of water and has been used in drug design to displace water molecules from the binding sites of proteins [27]. For example, the introduction of nitrile groups at the appropriate sites of quinazoline and benzotriazine inhibitors of scytalone dehydratase improved the inhibition potencies by several orders of magnitude [28]. To examine the potential role that

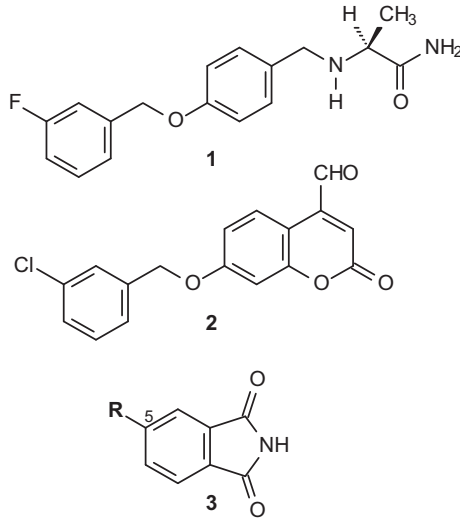

Fig. 1. The structures of safinamide (**1**), 7-(3-chlorobenzyloxy)-4-formylcoumarin (**2**) and C5-substituted phthalimide (**3**).

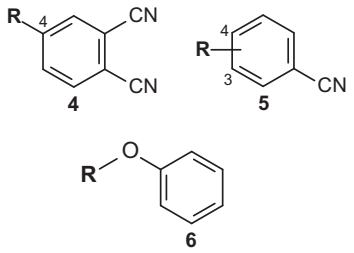

Fig. 2. The structures of C4-substituted phthalonitrile (**4**), C3- and C4-substituted benzonitriles (**5**) benzyl phenyl ether (**6**) analogues.

nitrile groups may play in the binding of the C4-substituted phthalonitriles to MAO-A and -B, a series of C3- and C4-substituted benzonitriles (**5**) were synthesized and examined as inhibitors. Furthermore, a series of homologs (**6**) devoid of the nitrile functional group was also investigated as potential MAO inhibitors. Similar to the C5-substituted phthalimides, alkyl- and aryloxy side chains were selected for the purpose of this study since these have been shown to enhance the MAO-A and -B binding affinities of a variety of scaffolds including caffeine, isatin and phthalimide [26,29,30]. Previous studies have suggested that alkyl- and aryloxy side chains, with a relatively larger degree of conformational freedom as a result of rotation about the carbon–oxygen ether bond, may be better suited for binding to MAO-A than relatively rigid structures [29,31]. Although intended for binding to MAO-B, the C4-substituted phthalonitriles examined here may therefore also act as MAO-A inhibitors.

2. Results

2.1. Chemistry

In the present study a series of C4-substituted phthalonitrile (**4a–i**), C3- and C4-substituted benzonitrile (**5a–h**) and benzyl phenyl ether analogs (**6a–d**) were synthesized with the aim of examining their MAO inhibitory properties. The target phthalonitrile analogs (**4a–i**) were synthesized by reacting 4-nitrophthalonitrile with the appropriate alcohol in the presence of potassium carbonate in dimethyl sulfoxide (DMSO) (Scheme 1) [32]. The phthalonitriles were in most cases obtained in relatively good yields (up to 84%). The substituted benzonitrile analogs (**5a–h**) investigated in this study were synthesized in a similar manner by reacting the 3- or 4-nitrobenzonitrile with an appropriate alcohol [32].

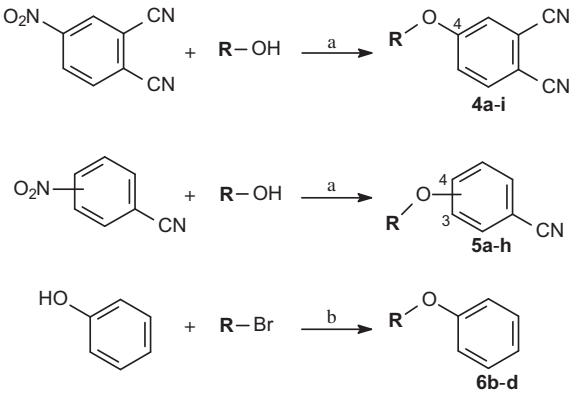

Scheme 1. Synthetic pathway to C4-substituted phthalonitrile analogues (**4a–i**), C3- and C4-substituted benzonitrile analogues (**5a–h**) and benzyl phenyl ether analogues (**6b–d**). Reagents and conditions: (a) K_2CO_3, DMSO, argon, (b) K_2CO_3, acetone.

For this reaction, yields of 22–61% were obtained. With the exception of **6a** which is commercially available, the benzyl phenyl ether analogs (**6b–d**) were synthesized by reacting phenol with an alkyl bromide in the presence of potassium carbonate in acetone. Yields of 54–67% were obtained. In each instance, the structures and purities of the new compounds were verified by ^{1}H NMR, ^{13}C NMR, mass spectrometry and HPLC analysis as cited in Section 4.

2.2. MAO inhibition studies

To examine the MAO inhibition potencies of the phthalonitrile (**4a–i**), benzonitrile (**5a–h**) and benzyl phenyl ether analogs (**6a–d**), recombinant human MAO-A and -B were employed as enzyme sources. As enzyme substrate the mixed MAO-A/B substrate, kynuramine, was used. Kynuramine, which exhibits similar K_m values towards the two enzymes (16.1 μM and 22.7 μM for MAO-A and -B, respectively) is oxidized to yield 4-hydroxyquinoline, a fluorescent compound which is readily measurable in the presence of the non-fluorescent substrate [29]. At the excitation and emission wavelengths (λ_{ex} = 310 nm, λ_{em} = 400 nm) and inhibitor concentrations used, none of the test inhibitors fluoresced, or quenched the fluorescence of 4-hydroxyquinoline. The inhibition potencies of the test inhibitors are expressed as the IC_{50} values which were determined from sigmoidal dose–response curves as shown by example in Fig. 3.

2.2.1. MAO-B inhibition studies

The MAO-B inhibition potencies of the C4-substituted phthalonitrile analogs (**4a–i**) are presented in Table 1. With the exception of **4a** (IC_{50} = 6.02 μM), all the phthalonitrile analogs were found to be exceptionally potent MAO-B inhibitors with IC_{50} values in the nM range (0.005–0.57 μM). It is significant that **4a** contains the shortest C4 substituent (–OC_6H_5) among the phthalonitrile analogs examined. Increasing the length of the C4 side chain by only one methylene unit (–$OCH_2C_6H_5$) yields compound **4b** with an IC_{50} value of 0.0079 μM. Compound **4b** is approximately 750 fold more potent as an MAO-B inhibitor than is **4a**. In fact, **4b** is the third most potent MAO-B inhibitor among the phthalonitrile analogs. Further increasing the length of the C4 side chain yields the phenylethoxy- and phenylpropoxy substituted homologs **5c** (IC_{50} = 0.018 μM) and **5d** (IC_{50} = 0.136 μM), which were also found to be potent MAO-B inhibitors. Also of significance is the observation that replacement of the phenoxy phenyl ring of **4a** with a naphthalenyl ring to yield compound **4f**, results in enhanced MAO-B inhibition potency. Compound **4f** (IC_{50} = 0.244 μM) is approximately 24 fold more potent than **4a** as an MAO-B inhibitor. This result reveals that increasing the size of the aromatic ring of the C4 substituent is also a strategy to enhance the MAO-B inhibition potencies of C4-substituted phthalonitrile analogs. The finding that increasing size or length of the C4 substituent leads to enhanced MAO-B inhibition will be explored with the aid of molecular modeling below. Interestingly, the introduction of an ethenyl double bond into the C4 side chain, as observed with the phenylpropenyloxy derivative **4e**, also resulted in potent MAO-B inhibition (IC_{50} = 0.0066 μM). In an attempt to further enhance the MAO-B inhibition potencies of the phthalonitrile analogs, the phenyl rings of the C4 substituent of selected homologs (**4a–c**) were substituted with bromine. It has previously been documented that bromine substitution on the phenyl rings of alkyloxy- and aryloxy substituted phthalimide analogs leads to further enhancement of binding to MAO-B [26]. The results show that bromine substitution of phthalonitrile **4a** (to yield **4g**) results in an IC_{50} value for the inhibition of MAO-B of 0.568 μM, 10 fold more potent than **4a** (IC_{50} = 6.02 μM). The bromine substituted homologs of **4b** and **4c** were also found to be potent MAO-B inhibitors with recorded IC_{50} values of 0.0048 μM for **4h** and 0.226 μM for **4i**. The bromine substituted compound **4h** is therefore only slightly more potent than its unsubstituted homolog **4b** (IC_{50} = 0.0079 μM) as an MAO-B inhibitor while **4i** is a weaker inhibitor than its unsubstituted homolog **4c** (IC_{50} = 0.018 μM). These results indicate that bromine substitution on the phenyl ring of the C4 substituent enhances the MAO-B inhibition potencies of weaker phthalonitrile inhibitors such as **4a** to a large degree while its effects on the MAO-B inhibition potencies of the more potent analogs (**4b**, **4c**) are less significant and may even lead to a loss of inhibition activity.

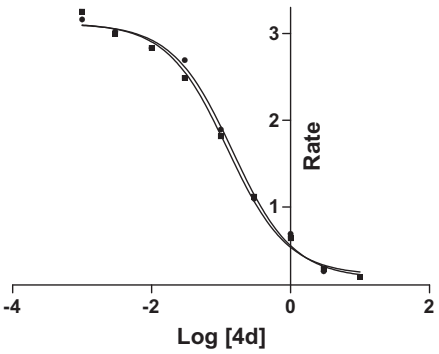

Fig. 3. The sigmoidal dose-response curve of the initial oxidation rate of human MAO-B vs. the logarithm of the concentration of **4d** (expressed in μM). The determinations were carried out in duplicate and the catalytic rates are expressed as nmoles 4-hydroxyquinoline formed/min/mg protein.

Table 1
The IC_{50} values for the inhibition of recombinant human MAO-A and -B by phthalonitrile analogues **4a–i**.[a]

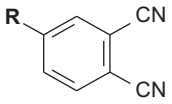

	IC_{50} (μM)			SI[b]
	R	MAO-A	MAO-B	
4a	C_6H_5O	25.2 ± 0.042	6.02 ± 0.33	4
4b	$C_6H_5CH_2O$	1.79 ± 0.016	0.0079 ± 0.001	227
4c	$C_6H_5CH_2CH_2O$	1.31 ± 0.059	0.018 ± 0.0003	73
4d	$C_6H_5(CH_2)_3O$	0.652 ± 0.067	0.136 ± 0.016	5
4e	(*E*)-$C_6H_5CH{=}CHCH_2O$	0.399 ± 0.026	0.0066 ± 0.0003	60
4f	2-Naphthalenyl-O	5.05 ± 0.113	0.244 ± 0.060	21
4g	4-BrC_6H_4O	19.2 ± 0.771	0.568 ± 0.055	34
4h	4-$BrC_6H_4CH_2O$	0.642 ± 0.217	0.0048 ± 0.0001	134
4i	4-$BrC_6H_4CH_2CH_2O$	2.45 ± 0.231	0.226 ± 0.019	11

[a] All values are expressed as the mean ± SD of duplicate determinations.
[b] The selectivity index is the selectivity for the MAO-B isoform and is given as the ratio of K_i(MAO-A)/K_i(MAO-B).

To examine the requirement of the presence of both nitrile groups of the phthalonitrile analogs for MAO-B inhibition, a series of benzonitriles (**5a–h**) was examined as MAO-B inhibitors. The importance of the position of the nitrile group on the phenyl ring with respect of the alkyloxy side chain was also investigated by synthesizing both the C3- and C4-substituted benzonitriles. The MAO inhibition potencies of the C3- and C4-substituted benzonitriles are presented in Table 2. Compounds **5a** and **5b**, the benzonitrile analogs of phthalonitrile **4b**, were both found to be weaker MAO-B inhibitors than **4b** (IC_{50} = 0.0079 μM) with IC_{50} values of 0.785 μM and 0.249 μM, respectively. Similarly, compounds **5c** and **5d**, the benzonitrile analogs of phthalonitrile **4e**, were also weaker MAO-B inhibitors than **4e** (IC_{50} = 0.0066 μM) with IC_{50} values of 0.376 μM and 0.174 μM, respectively. The same trend is observed for compounds **5e** (IC_{50} = 0.266 μM) and **5f** (IC_{50} = 0.041 μM) which were weaker MAO-B inhibitors than their

Table 2
The IC_{50} values for the inhibition of recombinant human MAO-A and -B by benzonitrile analogues **5a**–**h**.[a]

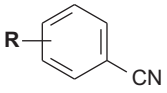

	IC_{50} (μM)			SI[b]
	R	MAO-A	MAO-B	
5a	4-$C_6H_5CH_2O$	32.2 ± 2.93	0.785 ± 0.049	41
5b	3-$C_6H_5CH_2O$	13.0 ± 2.95	0.249 ± 0.054	52
5c	4-(*E*)-$C_6H_5CH{=}CHCH_2O$	15.9 ± 0.636	0.376 ± 0.039	42
5d	3-(*E*)-$C_6H_5CH{=}CHCH_2O$	3.60 ± 0.565	0.174 ± 0.028	21
5e	4-(4-BrC_6H_4)CH_2O	2.44 ± 0.115	0.266 ± 0.004	9
5f	3-(4-BrC_6H_4)CH_2O	2.610 ± 0.173	0.041 ± 0.019	64
5g	4-(4-BrC_6H_4)CH_2CH_2O	11.85 ± 8.21	1.35 ± 0.074	9
5h	4-$C_6H_5CH_2O(CH_2)_2O$	69.5 ± 3.58	1.39 ± 0.322	50

[a] All values are expressed as the mean ± SD of duplicate determinations.
[b] The selectivity index is the selectivity for the MAO-B isoform and is given as the ratio of K_i(MAO-A)/K_i(MAO-B).

corresponding phthalonitrile analog **4h** (IC_{50} = 0.0048 μM). These results demonstrate that the phthalonitrile moiety is more optimal for MAO-B inhibition than the corresponding benzonitrile moiety. Also, the results show C3-substituted benzonitriles are better MAO-B inhibitors than C4-substituted benzonitriles. For example, C3-substituted benzonitrile **5b** is 3 fold more potent than its corresponding C4-substituted isomer **5a**, while **5d** is 2 fold more potent than its corresponding C4-substituted benzonitrile analog **5c**. Similarly, **5f**, is 6 fold more potent as a MAO-B inhibitor than its corresponding C4-substituted isomer **5e**. It may therefore be concluded that *meta* placement of the nitrile and alkyloxy groups results in more productive interactions with the MAO-B active site than *para* placement of these groups.

The significance of the nitrile functional groups for binding of the C4-substituted phthalonitriles to MAO-B was further investigated by examining the MAO-B inhibition potencies of a series of benzyl phenyl ether analogs (**6a**–**d**) which are devoid of the nitrile group. As shown in Table 3 the benzyl phenyl ether analogs proved to be moderately potent inhibitors of MAO-B with IC_{50} values in the μM range (1.3–11.8 μM). These inhibitors are therefore weaker MAO-B inhibitors when compared to the corresponding phthalonitriles and the benzonitriles which contain the same alkyloxy substituents. For example, the benzyloxy substituted phthalonitrile (**4b**) and benzonitriles (**5a** and **5b**) are 8–839 fold more potent as MAO-B inhibitors than benzyl phenyl ether (**6a**). As shown in Table 4, compounds **6b**–**d** were similarly weaker inhibitors than their nitrile containing homologs. From this result it may be concluded that the nitrile functional group is a requirement for high affinity binding of the phthalonitrile and benzonitrile analogs to the MAO-B active site.

Table 3
The IC_{50} values for the inhibition of recombinant human MAO-A and -B by analogues **6a**–**d**.[a]

		IC_{50} (μM)		SI[b]
		MAO-A	MAO-B	
6a	$C_6H_5CH_2O$ C_6H_5	No Inh.[c]	6.63 ± 0.59	–
6b	(*E*)-C_6H_5CH = $CHCH_2O$ C_6H_5	145 ± 18.5	1.32 ± 0.003	110
6c	(4-BrC_6H_4)CH_2O C_6H_5	65.5 ± 25.5	3.05 ± 0.487	21
6d	(4-BrC_6H_4) CH_2CH_2O C_6H_5	102 ± 12.0	11.8 ± 2.10	9

[a] All values are expressed as the mean ± SD of duplicate determinations.
[b] The selectivity index is the selectivity for the MAO-B isoform and is given as the ratio of K_i(MAO-A)/K_i(MAO-B).
[c] No inhibition observed at a maximal concentration of 100 μM of the test inhibitor.

2.2.2. MAO-A inhibition studies

As shown in Table 1 the C4-substituted phthalonitrile analogs (**4a**–**i**) are also inhibitors of human MAO-A. As evident from the selectivity index (SI) values all the phthalonitriles examined here are however selective inhibitors for the MAO-B isoform. The most selective inhibitor, compound **4b**, was 227 fold more selective for MAO-B than for MAO-A. In view of the high inhibition potency of **4b**, this compound may represent a promising MAO-B selective inhibitor. Although the phthalonitriles were weaker MAO-A inhibitors, several compounds displayed IC_{50} values in the nM range. For example, the most potent MAO-A inhibitor, compound **4e**, exhibited an IC_{50} value of 0.399 μM. Interestingly, similar to the results obtained with MAO-B, increasing the length of the C4 side chain was associated with an increase in MAO-A inhibition potency. For example, among the phthalonitriles, the phenoxy substituted homolog (**4a**) was the weakest MAO-A inhibitor with an IC_{50} value of 25.2 μM. Increasing the length of the C4 substituent yielded the benzyloxy (**4b**) and phenylethoxy (**4c**) substituted homologs with IC_{50} values of 1.79 μM and 1.31 μM, respectively. Further increasing the C4 side chain, as demonstrated by the phenylpropoxy (**4d**; IC_{50} = 0.652 μM) and phenylpropenyloxy (**4e**; IC_{50} = 0.399 μM) substituted homologs, yielded even more potent MAO-A inhibition. Bromine substitution on the phenyl ring of the C4 side chain did not enhance MAO-A inhibition activity to a large extent. For example, the bromine substituted analog **4h** exhibited an IC_{50} value for the inhibition of MAO-A of 0.642 μM, only 2.7 fold more potent than its unsubstituted homolog, **4b** (IC_{50} = 1.79 μM). Bromine substitution of **4a** and **4c**, to yield compounds **4g** and **4i**, was however associated with reduced MAO-A inhibition potency.

The C3- and C4-substituted benzonitrile analogs (**5a**–**h**) were also found to be MAO-A inhibitors (Table 2). Similar to the phthalonitriles, the benzonitriles were however selective inhibitors of the MAO-B isoform. In general, the series of benzonitriles were weaker MAO-A inhibitors than the corresponding phthalonitrile analogs. For example, compounds **5a** and **5b**, the benzonitrile analogs of phthalonitrile **4b** (IC_{50} = 1.79 μM) were relatively weak MAO-A inhibitors with IC_{50} values of 32.2 μM and 13.0 μM, respectively. Benzonitriles **5c** (IC_{50} = 15.9 μM) and **5d** (IC_{50} = 3.60 μM) were also weaker MAO-A inhibitors than their corresponding phthalonitrile analog **4e** (IC_{50} = 0.399 μM). The same trend was observed for the benzonitrile analogs **5e** and **5f** which were approximately 4 fold weaker MAO-A inhibitors that the corresponding phthalonitrile homolog **4h**. These results demonstrate that, as for MAO-B, the phthalonitrile moiety results in enhanced MAO-A inhibition compared to the corresponding benzonitrile moiety. In general, the C3-substituted benzonitriles were found to be more potent MAO-A inhibitors than the C4-substituted benzonitriles. For example, C3-substituted benzonitrile **5b** was found to be 2.5 fold more potent than the corresponding C4-substituted isomer **5a**, while **5d** was found to be 4 fold more potent than its corresponding C4-substituted isomer **5c**. The C4-substituted phthalonitrile **5e** and its C3-substituted isomer **5f** exhibited similar inhibition potencies towards MAO-A. Analogous to the inhibition results obtained with MAO-B, it may therefore be concluded that *meta* placement of the nitrile and alkyloxy groups, in general, may yield improved MAO-A inhibition activity compared to *para* placement of these groups.

The importance of the nitrile functional groups for interaction of the phthalonitrile and benzonitrile analogs with MAO-A was further investigated by determining the MAO-A inhibitory properties of the series of benzyl phenyl ether analogs (**6a**–**d**) which is devoid of the nitrile group (Table 3). Compared to the inhibition potencies of the phthalonitriles and benzonitriles, the benzyl phenyl ether analogs were found to be weak inhibitors of MAO-A with IC_{50} values ranging from 65.5 μM to 145 μM. Benzyl phenyl ether (**6a**) was found to be devoid of MAO-A inhibition properties. As shown in Table 4 the phthalonitrile (**4**) and benzonitrile (**5**) analogs

Table 4
A comparison of the IC_{50} values for the inhibition of MAO-B and -A by compounds **6** to the IC_{50} values of the corresponding compounds **4** and **5**.

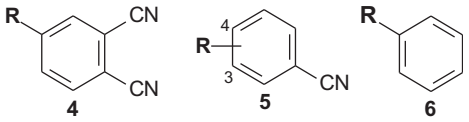

R	IC_{50} value ratios for the inhibition of MAO-B			IC_{50} value ratios for the inhibition of MAO-A		
	6/**4**[a]	**6**/**5**[b] (C4-subst.)	**6**/**5**[c] (C3-subst.)	**6**/**4**[a]	**6**/**5**[b] (C4-subst.)	**6**/**5**[c] (C3-subst.)
$C_6H_5CH_2O$	839	8	27	–	–	–
(*E*)-$C_6H_5CH{=}CHCH_2O$	200	4	8	363	9	40
4-$BrC_6H_4CH_2O$	635	11	74	102	27	25
4-$BrC_6H_4CH_2CH_2O$	52	9	–	42	9	–

[a] The ratio of the IC_{50} values of compounds **6** to the IC_{50} values of compounds **4**.
[b] The ratio of the IC_{50} values of compounds **6** to the IC_{50} values of compounds **5** containing C4 substituents.
[c] The ratio of the IC_{50} values of compounds **6** to the IC_{50} values of compounds **5** containing C3 substituents.

are 9–363 fold more potent as MAO-A inhibitors than the corresponding benzyl phenyl ether analogs (**6**). This analysis shows that the nitrile functional group significantly enhances the binding affinities of the substituted phthalonitrile and benzonitrile analogs to the MAO-A.

2.3. Reversibility of inhibition

Based on the highly potent MAO inhibition potencies of the phthalonitrile analogs, a selected phthalonitrile analog, compound **4d**, was evaluated for its ability to interact reversibly with human MAO-A and -B. For this purpose the time dependency of the inhibition was evaluated. While irreversible inhibitors would display a time-dependent reduction of enzyme activity, in the presence of reversible inhibitors enzyme activity would remain unchanged regardless of the time period for which the inhibitor is incubated with the enzyme. Compound **4d** was preincubated with recombinant human MAO-A or -B for various periods of time (0–60 min) and the residual MAO catalytic activities were measured after the addition of kynuramine to the incubations. The concentrations of **4d** that were selected for the preincubations were 1.31 μM and 0.27 μM for the incubations with MAO-A and -B, respectively. These concentrations are approximately 2 fold the measured IC_{50} values for the inhibition of the respective enzymes by **4d**. The results of these reversibility studies are presented in Fig. 4. As shown by the bar graphs, preincubation of **4d** with both MAO-A and -B does not result in a time-dependent loss of MAO-A and -B catalytic activities. Even after incubating **4d** for a period of 60 min with the MAO enzymes no reduction of the catalytic rates are observed. From these results it may therefore be concluded that **4d** is not a time-dependent inhibitor of MAO-A and -B and the interactions of this phthalonitrile analog with the MAO enzymes are reversible, at least for the time period (0–60 min) and at the inhibitor concentrations ($2 \times IC_{50}$) evaluated. Interestingly, a small but significant time-dependent increase of the MAO-A catalytic rate is observed when the enzyme is preincubated with **4d**. A plausible explanation for this behavior is not readily apparent.

To further examine the binding modes of **4d** to MAO-A and -B, the possibility that **4d** acts as a competitive inhibitor of these enzymes was explored. For this purpose, Lineweaver–Burk plots were constructed for the inhibition of MAO-A and –B by **4d**. The initial catalytic rates of MAO-A or -B were measured at four different concentrations (15–90 μM) of the substrate, kynuramine. These measurements were carried out in the absence and presence of three different concentrations of **4d**. For the studies with MAO-A the concentrations of **4d** were 0.1625–0.65 μM while for the studies with MAO-B the concentrations of **4d** were 0.035–0.14 μM. The

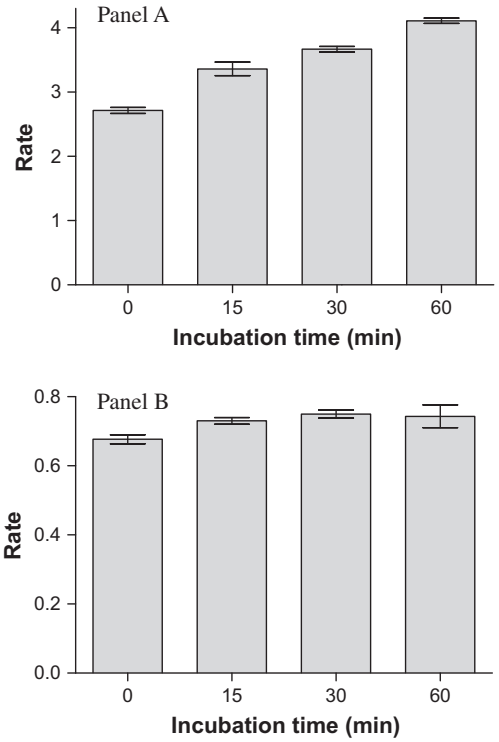

Fig. 4. The time-dependent inhibition of human MAO-A (Panel A) and MAO-B (Panel B) by **4d**. The enzymes were preincubated for various periods of time (0–60 min) with **4d** at concentrations of 1.31 μM and 0.27 μM for MAO-A and MAO-B, respectively, and the residual catalytic rated were recorded. The catalytic rates are expressed as nmoles 4-hydroxyquinoline formed/min/mg protein.

Lineweaver–Burk plots obtained in this manner are shown in Fig. 5. The results show that the sets of Lineweaver–Burk plots constructed for the inhibition of MAO-A and -B are linear and intersect at the *y*-axis. This indicates that the inhibition of the MAO enzymes by **4d** are competitive and thus provide further support that **4d** is a reversible MAO inhibitor.

2.4. Molecular modeling

To provide additional insight into the relationships between the MAO-A and -B inhibitory potencies and the structures of the inhibitors examined in this study, the binding modes of selected analogs (**4a**, **4b**, **5a** and **5b**) in the active site cavity of MAO-B and the

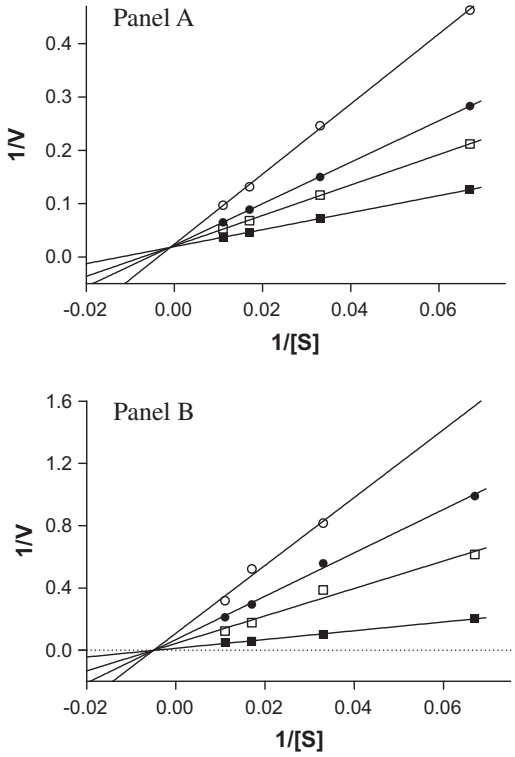

Fig. 5. Lineweaver-Burk plots of the catalytic rates of human MAO-A (Panel A) and MAO-B (Panel B) in the absence (filled squares) and presence of various concentrations of **4d**. For the studies with MAO-A (Panel A) the concentrations of **4d** were: 0.1625 μM (open squares), 0.325 μM (filled circles), 0.65 μM (open circles). For the studies with MAO-B (Panel B) the concentrations of **4d** were: 0.035 μM (open squares), 0.07 μM (filled circles), 0.14 μM (open circles). The catalytic rates (V) are expressed as nmol product formed/min/mg protein.

binding orientation of **4b** in the active site cavity of MAO-A were examined using molecular docking.

The Discovery Studio modeling software (Accelrys) [33] was used to carry out the molecular docking experiments according to a modification of a previously reported protocol (see Section 4) [29,30]. The three-dimensional structures of human MAO-A cocrystallized with harmine (PDB entry: 2Z5X) [22] and human MAO-B cocrystallized with safinamide (PDB entry: 2V5Z) [25] were selected for the modeling studies. The protonation states of the ionizable residues of the protein models were calculated and hydrogen atoms were added accordingly. The backbone atoms of the models were constrained and the models were subjected to an energy minimization cascade. For the purpose of the docking procedure the crystal waters were removed from the models with the exception of those in the MAO-A and -B active sites that are reported to be conserved and non-displaceable (see Section 4). The structures of ligands were constructed and prepared within Discovery Studio and were docked into the active sites of the MAO-A and -B models using the CDOCKER application. When redocking the structures of harmine and safinamide into the active sites of the enzymes, the docked binding orientations exhibited relatively small RMSD values of 0.77 Å and 1.66 Å, respectively, from the position of the cocrystallized ligands. This protocol may therefore be considered suitable for investigating the potential binding modes of inhibitors within MAO-A and -B.

The best ranked docking solution for the binding of **4b** to MAO-B illustrates that the phthalonitrile moiety of the structure binds within the substrate cavity while the alkyloxy side chain extends towards the entrance cavity. In the substrate cavity, the C1 nitrile group interacts via hydrogen bonding with the phenolic hydroxyl

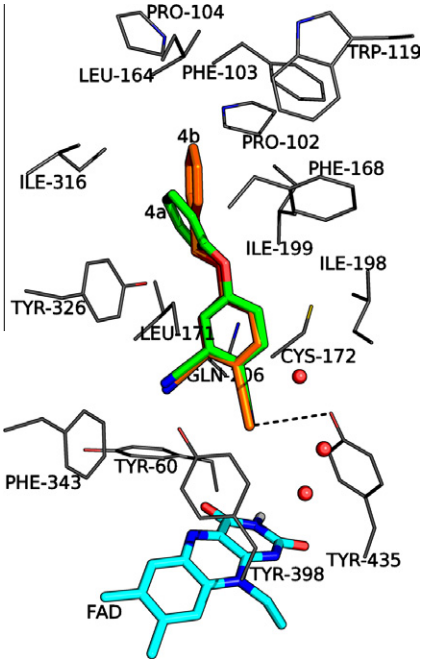

Fig. 6. An illustration of the predicted binding orientations of **4a** (green) and **4b** (orange) in the active site of MAO-B. (For interpretation of the references to color in this figure legend, the reader is referred to the web version of this article.)

group of Tyr-435 (Fig. 6). Interestingly, the C2 nitrile group is directed towards Tyr-60 and Phe-343 in a region of the substrate cavity that is considered to be relatively apolar [34]. No hydrogen bonding of the C2 nitrile is observed. Since the entrance cavity is a highly hydrophobic environment the alkyloxy side chain is most likely stabilized here via Van der Waals interactions [34]. Another potentially significant interaction is a π–sigma interaction between the alkyloxy side chain phenyl ring and Ile-199. The docked orientation of **4a** (Fig. 6) is similar to that of **4b** with the exception

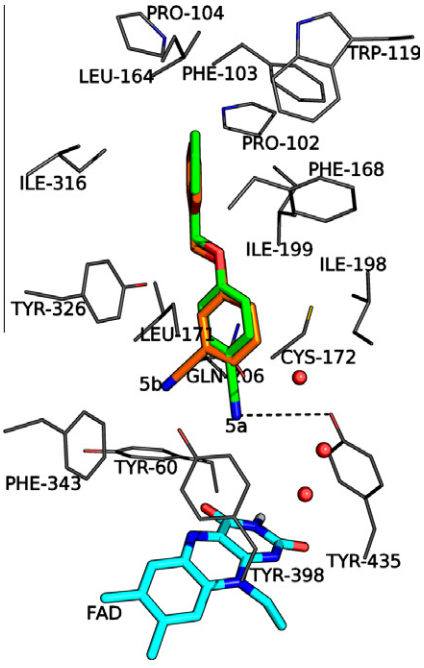

Fig. 7. An illustration of the predicted binding orientations of **5a** (green) and **5b** (orange) in the active site of MAO-B. (For interpretation of the references to color in this figure legend, the reader is referred to the web version of this article.)

than the aryloxy side chain of **4a** does not extend far into the entrance cavity and does not interact with Ile-199. The apparent reduced degree of interaction between the entrance cavity and the aryloxy side chain of **4a** may explain the relatively low binding affinity of this compound to MAO-B. The benzonitriles **5a** and **5b** adopt almost identical orientations to **4b** (Fig. 7). Similar to **4b**, the *para* nitrile group of **5a** undergoes a hydrogen bond interaction with the phenolic hydroxyl group of Tyr-435 while the *meta* nitrile group of **5b** is directed towards Tyr-60 and Phe-343, the hydrophobic patch in the substrate cavity. Even though no hydrogen bonding is predicted for the nitrile functional group of **5b**, the results of the enzyme inhibition studies showed that C3 substituted benzonitriles, such as **5b**, are more potent MAO-B inhibitors than the corresponding C4 substituted benzonitriles for which hydrogen bonding is predicted (e.g. **5a**). It may therefore be concluded that differing polar interactions of the C4 and C3 substituted benzonitriles with the substrate cavity do not account for the observed difference in MAO-B inhibition activities. It is noteworthy that similar binding orientations were generated using the LigandFit (Accelrys) [33] and GOLD (CCDC) [35] docking protocols (results not shown).

The predicted binding orientation of **4b** within the MAO-A active site shows that the phthalonitrile ring is bound to the substrate cavity where the C2 nitrile group is involved in hydrogen bonding with a crystal water molecule as well as with the phenolic hydroxyl of Tyr-444 (Fig. 8). In the MAO-A active site the phthalimide ring is rotated through approximately 180° compared to the orientation adopted in the MAO-B active site. This dissimilarity of the MAO-A and -B binding orientations of a specific inhibitor is frequently observed in docking studies. For example, the heterocyclic rings of caffeine [29] as well as isatin [30] derivatives are also rotated through ~180° when comparing the bound orientations in the MAO-B active site to those in the MAO-A active site. Although not involved in polar interactions the C1 nitrile group is located in close proximity to the FAD cofactor, approximately 3.0 Å from the carbonyl C4 of the FAD. The polar interactions of the C2 nitrile group appears to play a relatively large role in stabilizing the phthalimide inhibitors within the MAO-A active site and the loss of polar interactions between the nitrile groups and the substrate cavity may explain the reduction of the MAO-A inhibition potencies upon removal of the nitrile groups from the inhibitors. In the MAO-A active site, residue Phe-208 is located at the position occupied by Ile-199 in the MAO-B active site. As a result a π–sigma interaction, similar to that formed by the alkyloxy side chains with Ile-199 in the MAO-B active site, is not present between the inhibitors and the MAO-A active site. The loss of this interaction may explain, at least in part, the weaker MAO-A binding affinities of the phthalonitriles examined here compared to their corresponding MAO-B binding affinities.

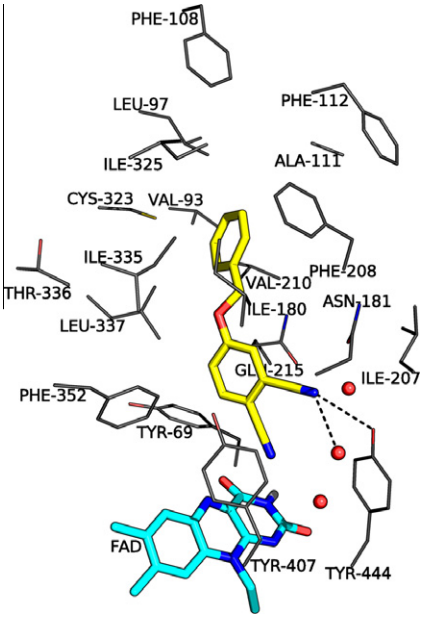

Fig. 8. An illustration of the predicted binding orientation of **4b** (yellow) in the active site of MAO-A. (For interpretation of the references to color in this figure legend, the reader is referred to the web version of this article.)

3. Discussion

In the present study it was shown that relatively simple small molecules may be endowed with potent MAO-B inhibition properties by appropriate substitution with the nitrile functional group. Phthalonitriles have been shown to be particularly potent reversible MAO-B inhibitors with all of the examined structures, except compound **4a**, possessing IC_{50} values in the nM range. Modeling studies suggest that the nitrile functional group interacts with the polar substrate cavity of the MAO-B enzyme while the alkyloxy side chain extends into the entrance cavity. This proposed dual binding has also been observed in MAO-B crystal structures containing other reversible inhibitors in the active site and may be a requirement for high affinity reversible interaction between the inhibitor and enzyme [24,25]. Structural modifications that lead to enhanced MAO-B inhibition potency include extending the length of the alkyloxy side chain and bromine substitution on the side chain phenyl ring. Both these modifications most probably lead to more productive interactions with the entrance cavity of MAO-B and hence more potent inhibition. Phthalonitrile analog **4a** possesses a relatively short alkyloxy side chain which does not project far into the entrance cavity and as a result may form only weak interactions with the enzyme entrance cavity. This may explain the relatively weak MAO-B inhibition potency of **4a** compared to the homologs containing longer alkyloxy side chains. Bromine substitution may have the same effect as lengthening the side chain or alternatively may promote dipole interactions within the entrance cavity thus leading to improved MAO-B inhibition.

The importance of the nitrile functional group for high affinity binding to MAO-B is demonstrated by the finding that removal of the nitrile groups is associated with a loss of MAO-B activity. As mentioned in the Introduction, the nitrile functional group is highly polar and probably interacts with the polar regions in the substrate cavity of the enzyme. Considering the high degree of loss of MAO-B activity (up to 839 fold) when the phthalonitrile nitrile groups are eliminated, the interactions formed by these groups are essential for stabilizing the phthalonitrile inhibitors in the MAO-B active site. These results show that substitution with a nitrile functional group may enhance the potency of reversible MAO-B inhibitors by several orders of magnitude, a strategy that may be applied in the design of MAO inhibitors. While the benzonitriles were weaker MAO-B inhibitors than the corresponding phthalonitriles they still exhibited high binding affinities to MAO-B, a property that may to a large degree be attributed to the presence of the remaining nitrile group.

Interestingly, the phthalonitriles were also found to be reversible MAO-A inhibitors although with weaker potencies compared to the inhibition of MAO-B. Phthalonitrile analogs **4d**, **4e** and **4h** exhibited IC_{50} values towards MAO-A in the nM range and since these compounds are also potent MAO-B inhibitors they represent potential leads for the design of mixed MAO-A/B inhibitors. The nitrile functional groups were also found to be a requirement for MAO-A inhibition since elimination of these groups results in loss

of activity. The active site cavities of MAO-A and -B are highly conserved with only 6 of the 16 active site residues differing between the two isoforms [22]. The polar regions of the MAO-A and -B active sites, in close proximity to the FAD, are in particular well conserved. It may therefore be expected that similar polar interactions between the MAO-A active site and the nitrile functional groups may form compared to those formed with the MAO-B active site. The proposed formation of these interactions may also explain the higher binding affinities of the phthalonitrile analogs compared to the corresponding analogs devoid of the nitrile functional group. Similar to the results obtained with MAO-B, the benzonitriles were weaker MAO-A inhibitors than the corresponding phthalonitriles. This result demonstrates that, as for MAO-B, the multiple nitrile groups cooperatively enhance binding affinity to MAO-A. The placement of the nitrile functional group on the phenyl ring of the benzonitrile inhibitors also affects MAO-A inhibition potency with *meta* placement of the nitrile and alkyloxy groups resulting in enhanced MAO-B inhibition compared to *para* placement of these groups.

4. Experimental section

4.1. Chemicals and instrumentation

Unless otherwise noted, all reagents were obtained from Sigma–Aldrich and were used without further purification. Benzyl phenyl ether (**6a**) was obtained from Sigma–Aldrich. Proton (^{1}H) and carbon (^{13}C) NMR spectra were recorded in DMSO-d6 with a Bruker Avance III 600 spectrometer at frequencies of 600 MHz and 150 MHz, respectively. The NMR chemical shifts are given as parts per million (δ) downfield from the signal of tetramethylsilane added to DMSO-d6 and spin multiplicities are given as s (singlet), d (doublet), dd (doublet of doublets), t (triplet) or m (multiplet). Direct insertion electron impact ionization (EI), atmospheric-pressure chemical ionization (APCI) and high resolution mass spectra (HRMS) were obtained on a DFS high resolution magnetic sector mass spectrometer (Thermo Electron Corporation) in electron ionization (EI) or atmospheric pressure chemical ionization (APCI) mode. Melting points (mp) were determined on a Stuart SMP10 melting point apparatus and are uncorrected. To estimate the degree of purity of the synthesized compounds, HPLC analyses were conducted with an Agilent 1100 HPLC system equipped with a quaternary pump and an Agilent 1100 series diode array detector (see Supplementary material). HPLC grade acetonitrile (Merck) and Milli-Q water (Millipore) were used for the chromatography. Fluorescence spectrophotometry was carried out with a Varian Cary Eclipse fluorescence spectrophotometer. Kynuramine.2HBr, 4-hydroxyquinoline and microsomes from insect cells containing recombinant human MAO-A and -B (5 mg/mL) were obtained from Sigma–Aldrich.

4.2. Synthesis of C4-substituted phthalonitrile analogs (**4a**–**i**)

The C4-substituted phthalonitrile analogs (**4a**–**i**) investigated in this study were synthesized according to the literature description [32]. In an atmosphere of argon, a mixture of 4-nitrophthalonitrile (17.5 mmol), the appropriate alcohol (21 mmol) and potassium carbonate (35 mmol) in 15 mL dimethyl sulfoxide (DMSO) was stirred at room temperature for a period of 48 h. The reaction was poured into 100 mL ice cold water and the precipitate was isolated by filtration and washed with 100 mL water. The crude material was dissolved in ethanol, filtered through cotton wool and left to recrystallize at room temperature. Purification of the target phthalonitriles required at least two successive rounds of recrystallization from ethanol.

4.2.1. 4-Phenoxyphthalonitrile (**4a**)

The title compound was prepared from 4-nitrophthalonitrile and phenol in a yield of 32%: mp 99–101 °C (ethanol), lit 100–101 °C [36]. ^{1}H NMR (DMSO-d6) δ 7.19 (d, 2H, J = 7.9 Hz), 7.32 (t, 1H, J = 7.5 Hz), 7.35 (dd, 1H, J = 2.6, 9.0 Hz), 7.50 (t, 2H, J = 8.3 Hz), 7.77 (d, 1H, J = 2.3 Hz), 8.08 (d, 2H, J = 8.7 Hz); ^{13}C NMR (DMSO-d6) δ 108.1, 115.4, 115.9, 116.7, 120.4, 121.89, 122.7, 125.9, 130.7, 136.3, 153.8, 161.1; APCI-MS 220; APCI-HRMS m/z: Calcd 220.0637. Found 220.0644; Purity (HPLC): 98.9%.

4.2.2. 4-Benzyloxyphthalonitrile (**4b**)

The title compound was prepared from 4-nitrophthalonitrile and benzyl alcohol in a yield of 84%: mp 104–106 °C (ethanol). ^{1}H NMR (DMSO-d6) δ 5.26 (s, 2H), 7.36 (t, 1H, J = 7.5 Hz), 7.41 (t, 2H, J = 7.9 Hz), 7.46 (d, 2H, J = 7.5 Hz), 7.52 (dd, 1H, J = 2.6, 8.7 Hz), 7.85 (d, 1H, J = 2.6 Hz), 8.05 (d, 1H, J = 9.0 Hz); ^{13}C NMR (DMSO-d6) δ 70.5, 106.1, 115.7, 116.2, 116.3, 120.5, 128.1, 128.4, 128.6, 135.4, 135.8, 161.7; EIMS 234; EI-HRMS m/z: Calcd 234.0793. Found 234.0794; Purity (HPLC): 98.4%.

4.2.3. 4-(2-Phenylethoxy)phthalonitrile (**4c**)

The title compound was prepared from 4-nitrophthalonitrile and 2-phenylethanol in a yield of 24%: mp 113–114 °C (ethanol). ^{1}H NMR (DMSO-d6) δ 3.06 (t, 2H, J = 6.8 Hz), 4.37 (t, 2H, J = 6.8 Hz), 7.22 (m, 1H), 7.31 (m, 4H), 7.44 (dd, 1H, J = 2.6, 9.0 Hz), 7.77 (d, 1H, J = 2.6 Hz), 8.02 (d, 1H, J = 9.0 Hz); ^{13}C NMR (DMSO-d6) δ 34.4, 69.4, 105.9, 115.7, 116.2, 116.3, 120.1, 120.3, 126.4, 128.3, 129.0, 135.7, 137.6, 161.8; APCI-MS 248; APCI-HRMS m/z: Calcd 248.0950. Found 248.0937; Purity (HPLC): 97.2%.

4.2.4. 4-(3-Phenylpropoxy)phthalonitrile (**4d**)

The title compound was prepared from 4-nitrophthalonitrile and 3-phenyl-1-propanol in a yield of 24%: mp 113–114 °C (ethanol). ^{13}C NMR (DMSO-d6) δ 2.03 (m, 2H), 2.72 (t, 2H, J = 7.5 Hz), 4.12 (t, 2H, J = 6.4 Hz), 7.17 (t, 1H, J = 7.5 Hz), 7.21 (d, 2H, J = 7.2 Hz), 7.27 (t, 2H, J = 7.5 Hz), 7.43 (dd, 1H, J = 2.6, 9.0 Hz), 7.75 (d, 1H, J = 2.6 Hz), 8.02 (d, 1H, J = 9.0 Hz); ^{13}H NMR (DMSO-d6) δ 29.9, 31.2, 68.3, 105.8, 115.8, 116.2, 116.3, 120.1, 120.3, 125.9, 128.3, 128.4, 135.8, 141.1, 162.0; APCI-MS 262; APCI-HRMS m/z: Calcd 262.1106. Found 262.1098; Purity (HPLC): 94.5%.

4.2.5. 4-{[(2E)-3-phenylprop-2-en-1-yl]oxy}phthalonitrile (**4e**)

The title compound was prepared from 4-nitrophthalonitrile and cinnamyl alcohol in a yield of 70%: mp 143–145 °C (ethanol). ^{1}H NMR (DMSO-d6) δ 4.89 (d, 2H, J = 6.0 Hz), 6.50 (m, 1H), 6.80 (d, 1H, J = 15.8 Hz), 7.27 (t, 1H, J = 7.2 Hz), 7.34 (t, 2H, J = 7.5 Hz), 7.49 (m, 3H), 7.82 (s, 1H), 8.05 (d, 1H, J = 8.7 Hz); ^{13}C NMR (DMSO-d6) δ 69.4, 106.0, 115.8, 116.2, 116.3, 120.4, 120.5, 123.3, 126.6, 128.2, 128.7, 133.8, 135.8, 161.6; EIMS 260; EI-HRMS m/z: Calcd 260.0950. Found 260.0946; Purity (HPLC): 92.9%.

4.2.6. 4-(Naphthalen-2-yloxy)phthalonitrile (**4f**)

The title compound was prepared from 4-nitrophthalonitrile and 2-naphthol in a yield of 76%: mp 121–123 °C (ethanol). ^{1}H NMR (DMSO-d6) δ 7.37 (dd, 1H, J = 2.6, 9.0 Hz), 7.47 (dd, 1H, J = 2.6, 9.0 Hz), 7.54 (m, 2H), 7.710 (d, 1H, J = 1.9 Hz), 7.88 (d, 1H, J = 2.3 Hz), 7.91 (d, 1H, J = 7.91 Hz), 7.99 (d, 1H, J = 7.91 Hz), 8.06 (d, 1H, J = 9.0 Hz), 8.11 (d, 1H, J = 8.7 Hz); ^{13}C NMR (DMSO-d6) δ 108.4, 115.4, 115.9, 116.7, 116.8, 120.0, 122.4, 123.0, 125.9, 127.0, 127.5, 127.8, 130.8, 130.9, 133.9, 136.3, 151.6, 161.1; APCI-MS 270; APCI-HRMS m/z: Calcd 270.0793. Found 270.0795; Purity (HPLC): 97.3%.

4.2.7. 4-(4-Bromophenoxy)phthalonitrile (**4g**)

The title compound was prepared from 4-nitrophthalonitrile and 4-bromophenol in a yield of 71%: mp 193–195 °C (ethanol).

^{1}H NMR (DMSO-d6) δ 7.17 (d, 2H, J = 9.0 Hz), 7.43 (dd, 1H, J = 2.6, 8.7 Hz), 7.66 (d, 2H, J = 8.7 Hz), 7.84 (d, 1H, J = 2.6 Hz), 8.10 (d, 1H, J = 2.6 Hz); ^{13}C NMR (DMSO-d6) δ 108.6, 115.3, 115.9, 116.8, 117.8, 122.4, 122.6, 122.9, 133.4, 136.3, 153.3, 160.6; APCI-MS 298, 300; APCI-HRMS m/z: Calcd 299.9721. Found 299.9725; Purity (HPLC): 99.8%.

4.2.8. 4-(4-Bromobenzyloxy)phthalonitrile (**4h**)

The title compound was prepared from 4-nitrophthalonitrile and 4-bromobenzyl alcohol in a yield of 44%: mp 144–145 °C (ethanol). ^{1}H NMR (DMSO-d6) δ 5.24 (s, 2H), 7.42 (d, 2H, J = 7.5 Hz), 7.51 (d, 1H, J = 8.7 Hz), 7.60 (d, 2H, J = 7.5 Hz), 7.84 (s, 1H), 8.06 (d, 1H, J = 8.7 Hz); ^{13}C NMR (DMSO-d6) δ 69.6, 106.3, 115.7, 115.8, 116.2, 116.3, 120.5, 121.6, 130.2, 131.5, 134.9, 135.8, 161.4; Purity (HPLC): 96.3%.

4.2.9. 4-[2-(4-Bromophenyl)ethoxy]phthalonitrile (**4i**)

The title compound was prepared from 4-nitrophthalonitrile and 2-(4-bromophenyl)ethanol in a yield of 7%: mp 103–105 °C (ethanol). ^{1}H NMR (DMSO-d6) δ 3.04 (t, 2H, J = 6.7 Hz), 4.35 (t, 2H, J = 6.7 Hz), 7.28 (d, 2H, J = 7.9 Hz), 7.43 (d, 1H, J = 8.7 Hz), 7.49 (d, 2H, J = 8.3 Hz), 7.76 (s, 1H), 8.01 (d, 1H J = 8.7 Hz); ^{13}C NMR (DMSO-d6) δ 33.7, 69.1, 106.0, 115.7, 116.2, 116.3, 119.6, 120.1, 120.3, 131.2, 131.3, 135.8, 137.2, 161.7; EIMS 326; EI-HRMS m/z: Calcd 326.0055. Found 326.0044; Purity (HPLC): 97.5%.

4.3. Synthesis of C3- and C4-substituted benzonitrile analogs (**5a**–**h**)

The substituted benzonitrile analogs (**5a**–**h**) investigated in this study were synthesized by reacting 3- or 4-nitrobenzonitrile with the appropriate alcohol according to the procedure described above for the synthesis of the phthalonitrile analogs (**4a**–**i**) [32].

4.3.1. 4-(Benzyloxy)benzonitrile (**5a**)

The title compound was prepared from 4-nitrobenzonitrile and benzyl alcohol in a yield of 47%: mp 96–98 °C (ethanol), lit 96 °C [37]. ^{1}H NMR (DMSO-d6) δ 5.19 (s, 2H), 7.17 (d, 2H, J = 9.0 Hz), 7.34 (t, 1H, J = 7.5 Hz), 7.39 (t, 2H, J = 7.9 Hz), 7.44 (d, 2H, J = 7.5 Hz), 7.76 (d, 2H, J = 9.0 Hz); ^{13}C NMR (DMSO-d6) δ 69.7, 103.0, 115.9, 119.1, 127.9, 128.1, 128.5, 134.2, 136.1, 161.8; EIMS 209; EI-HRMS m/z: Calcd 209.0841. Found 209.0844; Purity (HPLC): 99.2%.

4.3.2. 3-(Benzyloxy)benzonitrile (**5b**)

The title compound was prepared from 3-nitrobenzonitrile and benzyl alcohol in a yield of 43% (oil). ^{1}H NMR (DMSO-d6) δ 5.15 (s, 2H), 7.33 (m, 2H), 7.38 (t, 3H, J = 7.5 Hz), 7.45 (m, 3H), 7.49 (m, 1H); ^{13}C NMR (DMSO-d6) δ 69.6, 112.2, 117.7, 118.6, 120.5, 124.6, 127.8, 128.0, 128.5, 130.8, 136.3, 158.4; EIMS 209; EI-HRMS m/z: Calcd 209.0841. Found 209.0841; Purity (HPLC): 92.8%.

4.3.3. 4-{[(2E)-3-phenylprop-2-en-1-yl]oxy}benzonitrile (**5c**)

The title compound was prepared from 4-nitrobenzonitrile and cinnamyl alcohol in a yield of 34%: mp 117–118 °C (ethanol), lit 121 °C [38]. ^{1}H NMR (DMSO-d6) δ 4.83 (d, 2H, J = 5.6 Hz), 6.51 (m, 1H), 6.78 (d, 1H, J = 15.8 Hz), 7.17 (d, 2H, J = 9.0 Hz), 7.27 (t, 1H, J = 7.1 Hz), 7.35 (t, 2H, J = 7.1 Hz), 7.48 (d, 2H, J = 7.5 Hz), 7.78 (d, 2H, J = 8.7 Hz); ^{13}C NMR (DMSO-d6) δ 68.5, 102.9, 115.8, 119.1, 124.0, 126.5, 128.0, 128.7, 133.1, 134.2, 135.9, 161.7; Purity (HPLC): 91.5%.

4.3.4. 3-{[(2E)-3-phenylprop-2-en-1-yl]oxy}benzonitrile (**5d**)

The title compound was prepared from 3-nitrobenzonitrile and cinnamyl alcohol in a yield of 29% (yellow oil). ^{1}H NMR (DMSO-d6) δ 4.79 (d, 2H, J = 6.0 Hz), 6.50 (m, 1H), 6.77 (d, 1H, J = 16.2 Hz), 7.27 (t, 1H, J = 7.5 Hz), 7.34 (t, 3H, J = 7.5 Hz), 7.40 (d, 1H, J = 7.5 Hz), 7.49 (m, 4H); ^{13}C NMR (DMSO-d6) δ 68.5, 112.2, 117.7, 118.7, 120.6, 124.2, 124.6, 126.5, 128.0, 128.7, 130.9, 133.0, 136.0, 158.4; Purity (HPLC): 90.5%.

4.3.5. 4-(4-Bromobenzyloxy)benzonitrile (**5e**)

The title compound was prepared from 4-nitrobenzonitrile and 4-bromobenzyl alcohol in a yield of 22%: mp 118–120 °C (ethanol), lit 130–131 °C [39]. ^{1}H NMR (DMSO-d6) δ 5.18 (s, 2H), 7.16 (d, 2H, J = 8.7 Hz), 7.40 (d, 2H, J = 8.7 Hz), 7.58 (d, 2H, J = 8.3 Hz), 7.76 (d, 2H, J = 8.7 Hz); ^{13}C NMR (DMSO-d6) δ 68.8, 103.1, 115.9, 119.1, 121.3, 130.0, 131.4, 134.2, 135.6, 161.6; EIMS 287; EI-HRMS m/z: Calcd 286.9946. Found 286.9953; Purity (HPLC): 98.9%.

4.3.6. 3-(4-Bromobenzyloxy)benzonitrile (**5f**)

The title compound was prepared from 3-nitrobenzonitrile and 4-bromobenzyl alcohol in a yield of 29%: mp 78–79 °C (ethanol). ^{1}H NMR (DMSO-d6) δ 5.15 (s, 2H), 7.35 (dd, 1H, J = 2.3, 8.3 Hz), 7.41 (d, 3H, J = 8.3 Hz), 7.48 (d, 1H, J = 8.3 Hz), 7.50 (s, 1H), 7.59 (d, 2H, J = 8.3 Hz); ^{13}C NMR (DMSO-d6) δ 68.8, 112.2, 117.7, 118.6, 120.6, 121.2, 124.8, 130.0, 130.9, 131.4, 135.8, 158.2; EIMS 287; EI-HRMS m/z: Calcd 286.9946. Found 286.9951; Purity (HPLC): 98.1%.

4.3.7. 4-[2-(4-Bromophenyl)ethoxy]benzonitrile (**5g**)

The title compound was prepared from 4-nitrobenzonitrile and 2-(4-bromophenyl)ethanol in a yield of 61%: mp 80–81 °C (ethanol). ^{1}H NMR (DMSO-d6) δ 3.01 (t, 2H, J = 6.8 Hz), 4.25 (t, 2H, J = 6.8 Hz), 7.07 (d, 2H, J = 8.7 Hz), 7.27 (d, 2H, J = 8.3 Hz), 7.47 (d, 2H, J = 8.3 Hz), 7.72 (d, 2H, J = 9.0 Hz); ^{13}C NMR (DMSO-d6) δ 34.0, 68.3, 102.9, 115.7, 119.3, 119.6, 131.3, 131.4, 134.3, 137.7, 161.9; Purity (HPLC): 98.4%.

4.3.8. 4-[2-(Benzyloxy)ethoxy]benzonitrile (**5h**)

The title compound was prepared from 4-nitrobenzonitrile and 2-benzyloxyethanol in a yield of 24% (oil). ^{1}H NMR (DMSO-d6) δ 3.77 (t, 2H, J = 4.5 Hz), 4.22 (t, 2H, J = 4.5 Hz), 4.54 (s, 2H), 7.11 (d, 2H, J = 8.7 Hz), 7.27 (m, 1H), 7.32 (m, 4H), 7.74 (d, 2H, J = 8.7 Hz); ^{13}C NMR (DMSO-d6) δ 67.6, 67.9, 72.1, 102.8, 115.6, 119.1, 127.4, 127.5, 128.2, 134.1, 138.2, 162.0; EIMS 253; EI-HRMS m/z: Calcd 253.1103. Found 253.1111; Purity (HPLC): 90.4%.

4.4. Synthesis of benzyl phenyl ether analogs (**6a**–**d**)

While benzyl phenyl ether (**6a**) is commercially available (Sigma–Aldrich), analogs **6b**–**d** were synthesized as follows: Phenol (0.01 mmol) and an appropriate alkyl bromide (0.01 mmol; cinnamyl bromide, 4-bromobenzyl bromide and 4-bromophenethyl bromide for the synthesis of **6b**, **6c** an **6d**, respectively) were dissolved in 40 mL dry acetone and K_2CO_3 (0.01 mmol) was added. The reaction mixture was heated under reflux for 48 h, filtered while hot and the residual K_2CO_3 was washed with acetone (10 mL). The filtrate was cooled to room temperature and concentrated under reduced pressure. The resulting residue was recrystallized twice from ethanol to yield the target ethers [40].

4.4.1. {[(2E)-3-phenylprop-2-en-1-yl]oxy}benzene (**6b**)

The title compound was prepared from phenol and cinnamyl bromide in a yield of 67%: mp 66–68 °C (ethanol), lit 68 °C [38]. ^{1}H NMR (DMSO-d6) δ 4.71 (d, 2H, J = 5.6 Hz), 6.51 (m, 1H), 6.75 (d, 1H, J = 16.2 Hz), 6.93 (t, 1H, J = 7.5 Hz), 6.99 (d, 2H, J = 7.9 Hz), 7.29 (m, 3H), 7.34 (t, 2H, J = 7.9 Hz), 7.47 (d, 2H, J = 7.5 Hz); ^{13}C NMR (DMSO-d6) δ 67.9, 114.7, 120.6, 125.0, 126.4, 127.9, 128.7, 129.5, 132.3, 136.2, 158.2; Purity (HPLC): 99.5%.

4.4.2. 1-Bromo-4-(phenoxymethyl)benzene (**6c**)

The title compound was prepared from phenol and 4-bromobenzyl bromide in a yield of 58%: mp 96–98 °C (ethanol), lit 92.5–93.5 °C [41]. ^{1}H NMR (DMSO-d6) δ 5.06 (s, 2H), 6.93 (t, 1H, J = 7.5 Hz), 6.98 (d, 2H, J = 8.3 Hz), 7.28 (t, 2H, J = 7.5 Hz), 7.39 (d, 2H, J = 7.9 Hz), 7.56 (d, 2H, J = 8.3 Hz); ^{13}C NMR (DMSO-d6) δ 68.2, 114.8. 120.8, 120.9, 129.5, 129.7, 131.3, 136.6, 158.1; Purity (HPLC): 99.5%.

4.4.3. 1-Bromo-4-(2-phenoxyethyl)benzene (**6d**)

The title compound was prepared from phenol and 4-bromophenethyl bromide in a yield of 54% (yellow oil). ^{1}H NMR (DMSO-d6) δ 2.99 (t, 2H, J = 6.8 Hz), 4.15 (t, 2H, J = 2.8 Hz), 6.90 (m, 3H), 7.26 (t, 2H, J = 8.3 Hz), 7.29 (d, 2H, J = 8.3 Hz), 7.49 (d, 2H, J = 8.3 Hz); ^{13}C NMR (DMSO-d6) δ 34.2, 67.6, 114.4, 119.4, 120.6, 129.5, 131.1, 131.3, 138.0, 158.3; Purity (HPLC): 97.1%.

4.5. IC_{50} determinations for the inhibition of human MAO

Microsomes containing recombinant human MAO-A and -B (5 mg/mL) were pre-aliquoted and stored at −70 °C. Enzymatic reactions were prepared in potassium phosphate buffer (100 mM, pH 7.4, made isotonic with KCl) and contained kynuramine at concentrations of 45 μM and 30 μM for the incubations with MAO-A and -B, respectively. Various concentrations of the test inhibitor (0–100 μM) were added and the reactions were initiated with the addition of the MAO enzymes (0.0075 mg/mL). All stock solutions of the test inhibitors were prepared in DMSO and added to the reactions to yield a final concentration of 4% (v/v) DMSO. The final volumes of the reactions were 500 μL. The reactions were allowed to incubate for 20 minutes at 37 °C and were terminated with the addition of 200 μL NaOH (2 N) and 1200 μL distilled water. The reactions were centrifuged for 10 min at 16,000*g* and the fluorescence of the MAO generated 4-hydroxyquinoline in the supernatant fractions were measured (λ_{ex} = 310 nm, λ_{em} = 400 nm) [42]. The concentrations of 4-hydroxyquinoline were determined with a linear calibration curve constructed from solutions of authentic 4-hydroxyquinoline (0.047–1.50 μM). The calibration standards were prepared to a volume of 500 μL in potassium phosphate buffer and contained 4% DMSO. To each standard was added 200 μL NaOH (2 N) and 1200 μL distilled water. IC_{50} values were determined by graphing the initial MAO catalytic rates versus the logarithm of the inhibitor concentration to obtain a sigmoidal dose–response curve. Each curve was constructed from nine different inhibitor concentrations spanning at least three orders of magnitude. These data were fitted to the one site competition model (GraphPad Prism) and the IC_{50} values were determined in duplicate and are expressed as mean ± standard deviation (SD) [29].

4.6. Time-dependent inhibition studies

To examine the reversibility of MAO inhibition, time-dependent inhibition studies were carried with **4d** as selected inhibitor. All preincubations and incubations were carried out in potassium phosphate buffer (100 mM, pH 7.4, made isotonic with KCl). Compound **4d**, at concentrations of 1.31 μM and 0.27 μM for MAO-A and -B, respectively, were preincubated with the enzymes (0.03 mg/mL) for periods of 0, 15, 30, 60 min at 37 °C. These concentrations of **4d** are 2 fold the measured IC_{50} values for the inhibition of the respective MAO enzymes. Kynuramine at concentrations of 45 μM and 30 μM for the incubations with MAO-A and -B, respectively, were then added to the preincubations to yield a final enzyme concentration of 0.015 mg/mL. The resulting reactions (500 μL final volume) were incubated at 37 °C for 15 minutes. The final concentrations of **4d** were 0.655 μM and 0.135 μM for MAO-A and MAO-B, respectively, which are approximately equal to the IC_{50} values for the inhibition of the respective enzymes by **4d**. The reactions were terminated with the addition of 200 μL NaOH (2 N) and 1200 μL distilled water and the rates of formation of 4-hydroxyquinoline were measured as described above. All measurements were carried out in triplicate and are expressed as mean ± SD [29,30].

4.7. Construction of Lineweaver–Burk plots

Sets of Lineweaver–Burk plots were constructed for the inhibition of MAO-A and -B by a selected inhibitor, compound **4d**. The initial MAO catalytic rates were measured at four different kynuramine concentrations (15–90 μM), firstly in the absence of inhibitor and then in the presence of three different concentrations of **4d**. For this purpose the concentrations of **4d** were 0.1625–0.65 μM and 0.035–0.14 μM for the inhibition studies with MAO-A and -B, respectively. The concentrations of recombinant human MAO-A and -B used for these measurements were 0.015 mg/mL. All enzymatic reactions and measurements were carried out as described above. Linear regression analysis was performed using GraphPad Prism [29,30].

4.8. Molecular modeling studies

Molecular docking and manipulations of protein models were carried out in the Windows based Discovery Studio 1.7 molecular modeling software (Accelrys) [33]. The test ligands were constructed within Discovery Studio, the hydrogen atoms were added according to the appropriate protonation states at pH 7.4 and the geometries were briefly optimized in Discovery Studio using a Dreiding-like forcefield (5000 iterations). The ligands were subsequently prepared for the docking simulations utilizing the Prepare Ligands application of Discovery Studio and atom potential types and partial charges were assigned with the Momany and Rone CHARMm forcefield. The X-ray crystallographic structures of MAO-A cocrystallized with harmine (PDB code: 2Z5X) [22] and MAO-B cocrystallized with safinamide (PDB code: 2V5Z) [25] were obtained from the Brookhaven Protein Data Bank (www.rcsb.org/pdb). The protonation states of the ionizable amino acids residues were calculated at pH 7.4 and hydrogen atoms were added accordingly to the protein models. The valences of the FAD cofactors (oxidized state) and cocrystallized ligands were corrected and the models were automatically typed with the Momany and Rone CHARMm forcefield. After a fixed constraint was applied to the protein backbone, the models were energy minimized using the Smart Minimizer algorithm. The Smart Minimizer algorithm performs a steepest descent minimization (1000 steps) with a RMS gradient tolerance of 3, followed by conjugate gradient minimization. For this procedure the implicit generalized Born solvation model with molecular volume was used with the dielectric constant set to 4. The cocrystallized ligands and the backbone constraints were subsequently deleted from the models and the binding sites were identified by a flood-filling algorithm. In both the MAO-A and -B protein models, the cocrystallized water molecules were deleted with the exception of three active site waters. Since structures of MAO-B have shown that three active site water molecules (HOH 1155, 1170 and 1351; A-chain of 2V5Z) are conserved, all in the vicinity of the FAD cofactor they were retained for the simulations [25]. In the MAO-A structure, the crystal waters which occupy the analogous positions in the MAO-A active site (HOH 710, 718 and 739; 2Z5X) to those waters in the MAO-B active site cited above were retained. Docking was subsequently carried out with the CDOCKER protocol allowing for the generation of 10 random ligand conformations and a heating target temperature of 700 K in full potential mode. The docked ligands were finally

refined, using in situ ligand minimization, employing the Smart Minimizer algorithm. Unless otherwise specified (see above), all the application modules within Discovery Studio were set to their default values. The illustrations were generated with PyMOL [43].

Acknowledgments

The NMR spectra were recorded by André Joubert of the SASOL Centre for Chemistry, North-West University while the MS spectra were recorded by Marelize Ferreira of the Mass Spectrometry Service, University of the Witwatersrand. This work was supported by grants from the National Research Foundation and the Medical Research Council, South Africa.

Appendix A. Supplementary material

Supplementary data associated with this article can be found, in the online version, at doi:10.1016/j.bioorg.2011.10.003.

References

[1] M.B.H. Youdim, Y.S. Bakhle, Brit. J. Pharmacol. 147 (2006) S287–S296.
[2] M.B.H. Youdim, D.E. Edmondson, K.F. Tipton, Nat. Rev. Neurosci. 7 (2006) 295–309.
[3] A.A. Boulton, Prog. Neuropsychopharmacol. Biol. Psychiatry 15 (1991) 139–156.
[4] M.B.H. Youdim, M. Weinstock, Neurotoxicology 25 (2004) 243–250.
[5] P. Riederer, L. Lachenmayer, G. Laux, Curr. Med. Chem. 11 (2004) 2033–2043.
[6] A.-M. O'Carroll, C.J. Fowler, J.P. Phillips, I. Tobbia, K.F. Tipton, Naunyn Schmiedeberg's Arch. Pharmacol. 322 (1983) 198–202.
[7] K.N. Westlund, R.M. Denney, L.M. Kochersperger, R.M. Rose, C.W. Abell, Science 230 (1985) 181–183.
[8] S.E. Zisook, Psychosomatics 26 (1985) 240–251.
[9] P. Riederer, M.B.H. Youdim, J. Neurochem. 46 (1986) 1359–1365.
[10] H.H. Fernandez, J.J. Chen, Pharmacotherapy 27 (2007) 174S–185S.
[11] J.P. Finberg, J. Wang, K. Bankiewich, J. Harvey-White, I.J. Kopin, D.S. Goldstein, J. Neural Transm. Suppl. 52 (1998) 279–285.
[12] D.A. Di Monte, L.E. DeLanney, I. Irwin, J.E. Royland, P. Chan, M.W. Jacowec, J.W. Langston, Brain Res. 738 (1996) 53–59.
[13] P.A. LeWitt, D.C. Taylor, Neurotherapeutics 5 (2008) 210–225.
[14] M. Gesi, A. Santinami, R. Ruffoli, G. Conti, F. Fornai, Pharmacol. Toxicol. 89 (2001) 217–224.
[15] F. Fornai, G. Battaglia, M. Gesi, F.S. Giorgi, F. Orzi, F. Nicoletti, Brain Res. 887 (2000) 110–117.
[16] S.A. Marchitti, R.A. Deitrich, V. Vasiliou, Pharmacol. Rev. 59 (2007) 125–150.
[17] B. Halliwell, J. Neurochem. 59 (1992) 1609–1623.
[18] I. Lamensdorf, G. Eisenhofer, J. Harvey-White, A. Nechustan, K. Kirk, I.J. Kopin, Brain Res. 868 (2000) 191–201.
[19] A. Nicotra, F. Pierucci, H. Parvez, O. Santori, Neurotoxicology 25 (2004) 155–165.
[20] J.S. Fowler, N.D. Volkow, G.J. Wang, J. Logan, N. Pappas, C. Shea, R. MacGregor, Neurobiol. Aging 18 (1997) 431–435.
[21] R.N. Kalaria, M.J. Mitchell, S.I. Harik, Brain 111 (1988) 1441–1451.
[22] S.-Y. Son, J. Ma, Y. Kondou, M. Yoshimura, E. Yamashita, T. Tsukihara, Proc. Natl Acad. Sci. USA 105 (2008) 5739–5744.
[23] C. Binda, P. Newton-Vinson, F. Hubálek, D.E. Edmondson, A. Mattevi, Nat. Struct. Biol. 9 (2002) 22–26.
[24] F. Hubálek, C. Binda, A. Khalil, M. Li, A. Mattevi, N. Castagnoli, D.E. Edmondson, J. Biol. Chem. 280 (2005) 15761–15766.
[25] C. Binda, J. Wang, L. Pisani, C. Caccia, A. Carotti, P. Salvati, D.E. Edmondson, A. Mattevi, J. Med. Chem. 50 (2007) 5848–5852.
[26] C.I. Manley-King, J.J. Bergh, J.P. Petzer, Bioorg. Med. Chem. 19 (2011) 4829–4840.
[27] N.A. Meanwell, J. Med. Chem. 54 (2011) 2529–2591.
[28] J.M. Chen, S.L. Xu, Z. Wawrzak, G.S. Basarab, D.B. Jordan, Biochemistry 37 (1998) 17735–17744.
[29] B. Strydom, S.F. Malan, N. Castagnoli Jr., J.J. Bergh, J.P. Petzer, Bioorg. Med. Chem. 18 (2010) 1018–1028.
[30] C.I. Manley-King, J.J. Bergh, J.P. Petzer, Bioorg. Med. Chem. 19 (2011) 261–274.
[31] E.M. Van der Walt, E.M. Milczek, S.F. Malan, D.E. Edmondson, N. Castagnoli, J.J. Bergh, J.P. Petzer, Bioorg. Med. Chem. Lett. 19 (2009) 2509–2513.
[32] P. Tau, T. Nyokong, Electrochim. Acta 52 (2007) 3641–3650.
[33] Accelrys Discovery Studio 1.7, Accelrys Software Inc., San Diego, CA, USA. 2006. <http://www.accelrys.com>.
[34] L. Novaroli, A. Daina, E. Favre, J. Bravo, A. Carotti, F. Leonetti, M. Catto, P.A. Carrupt, M. Reist, J. Med. Chem. 49 (2006) 6264–6272.
[35] GOLD 5.0, Cambridge Crystallographic Data Center, Cambridge UK. 2010. <http://www.ccdc.cam.ac.uk>.
[36] X.-F. Zhang, Y. Wang, L. Niu, J. Photochem. Photobiol., A 209 (2010) 232–237.
[37] K.H. Baggaley, R. Fears, R.M. Hindley, B. Morgan, E. Murrell, D.E. Thorne, J. Med. Chem. 20 (1977) 1388–1393.
[38] G. Zahl, W. Kosbahn, G. Kresze, Liebigs Ann. Chem. (1975) 1733–1743.
[39] J. Dowden, P.D. Edwards, S.S. Flack, J.D. Kilburn, Chem-Eur. J. 5 (1999) 79–89.
[40] W.N. White, W.K. Fife, J. Am. Chem. Soc. 183 (1961) 3846–3853.
[41] R.C. Huston, A. Neeley, B.L. Fayerweather, H.M. D'Arcy, F.H. Maxfield, M.M. Ballard, W.C. Lewis, J. Am. Chem. Soc. 55 (1933) 2146–2149.
[42] L. Novaroli, M. Reist, E. Favre, A. Carotti, M. Catto, P.A. Carrupt, Bioorg. Med. Chem. 13 (2005) 6212–6217.
[43] W.L. DeLano, The PyMOL Molecular Graphics System, DeLano Scientific, San Carlos, USA, 2002.